

Depth-Dynamics Signatures of Conversational Collapse: Finite-Time Lyapunov Analysis of Transformer Forward Passes

Sohail Mohammad
Independent Researcher
`sohailmo.ai@gmail.com`

February 2026

Abstract

We estimate the top-1 finite-time Lyapunov exponent (λ_1) for transformer depth dynamics using forward-mode automatic differentiation (JVP-based tangent propagation) with QR renormalization, and test whether depth-dynamics summaries are associated with conversational collapse behavior observed in multi-turn self-play. Across 720 preregistered trajectories (4 conditions \times 36 seeds \times 5 repeats) and 7,200 FTLE computations on three 7B-parameter model families, we observe that λ_1 *profile features*—specifically the depth-profile slope ($\rho = -0.536$) and layerwise variance ($\rho = +0.511$)—show medium-to-large associations with collapse metrics from Escape Velocity. Mean λ_1 alone shows only weak association ($|\rho| \leq 0.25$). Three of six preregistered Spearman correlations pass the effect-size threshold ($|\rho| \geq 0.40$, Bonferroni–Holm adjusted $p < 0.05$), meeting the preregistered success criterion. However, the 720-row analysis contains only 108 unique λ_1 predictor vectors (36 seeds \times 3 distinct models), so nominal p -values are anti-conservative and effect-size magnitudes should be treated as the primary evidence. We interpret this as exploratory support for a bridge hypothesis, not confirmatory relationship establishment. All findings are predictive associations; no causal or mechanistic identity is claimed. Escape Velocity collapse labels have unconfirmed inter-rater reliability ($\kappa = 0.566$, threshold 0.80 not met), and this caveat applies to all bridge correlations.

1 Introduction

Transformer language models process input through a sequence of residual-stream updates across layers. This depth-wise computation can be viewed as a discrete dynamical system [Chen et al., 2018]: each layer maps the hidden state to a new state, accumulating nonlinear transformations. The sensitivity of this process to perturbations—quantified by Lyapunov exponents [Eckmann and Ruelle, 1985, Wolf et al., 1985]—provides a model-intrinsic characterization of how information is amplified or suppressed during a forward pass.

Separately, multi-turn self-play between language models exhibits *conversational collapse*: a progressive loss of output novelty where models become trapped in repetitive response patterns [Holtzman et al., 2019, Welleck et al., 2020, Li et al., 2016]. Escape Velocity characterized collapse dynamics across four interaction conditions using 7B-parameter models, achieving full confirmatory closure (720/720 trajectories) but not meeting its preregistered detector reliability threshold ($\kappa = 0.566$; threshold 0.80).

This paper asks whether the depth dynamics of a single forward pass—specifically, the top-1 finite-time Lyapunov exponent (λ_1)—are associated with the across-turn collapse behavior documented in Escape Velocity. This is a *predictive association* hypothesis: we test whether models

whose depth dynamics exhibit certain profile features tend to collapse more in extended conversations. We do not claim causal or mechanistic identity between within-pass depth dynamics and across-turn conversational dynamics, as these operate on fundamentally different time axes.

The primary contributions are: (1) a computationally feasible FTLE profiling pipeline for production-scale transformers; (2) preregistered evidence of observed conditional associations between depth-profile features and collapse metrics; and (3) transparent documentation of the structural limitations (predictor non-independence, inherited label uncertainty) that constrain inferential strength.

2 Methods

2.1 FTLE estimator

Let F_l denote the residual-stream update at layer l for a fixed token-context state. The local Jacobian $J_l = \partial F_l / \partial h_l$ characterizes sensitivity at each layer. Rather than computing full Jacobians (prohibitive for $d_{\text{model}} = 4096$), we use forward-mode automatic differentiation (JVP) [Baydin et al., 2018] to propagate tangent vectors through the layer stack.

Given an initial tangent vector v_0 , the tangent product $P_L v_0 = J_L \cdots J_2 J_1 v_0$ is computed via a single forward pass with `torch.func.jvp`. To prevent numerical overflow across 32 layers, we apply QR-based renormalization at a cadence of 4 layers (locked from Phase 1 pilot):

$$\lambda_1 = \frac{1}{L} \sum_{k=1}^{L/c} \log \|v_{kc}\| \quad \text{where } v_{kc} \text{ is renormalized every } c = 4 \text{ layers.} \quad (1)$$

For each trajectory, we compute λ_1 using 10 random tangent seeds (seeds 0–9) and report the mean across seeds. The layerwise λ_1 profile (log growth rate at each layer) captures the *shape* of sensitivity across depth.

2.2 Computation details

- **Token position:** Mean over all assistant tokens in the first turn.
- **Precision:** float32 throughout (locked after Phase 0 dtype transfer analysis showing float64 \leftrightarrow float32 $r = 0.788$; precisions are not interchangeable).
- **RoPE handling:** Non-GPT2 models (Llama, Qwen, Mistral) require explicit `position_embeddings` through JVP; fixed during Phase 0.
- **Flash attention:** Forced MATH SDPA backend (flash attention lacks forward-mode AD support).
- **Hardware:** Modal A100-80GB, max 2 concurrent containers per model.

2.3 Models and conditions

HETERO_ROT uses the first assistant model (Llama) for FTLE computation. HOMO_A and HETERO_ROT therefore produce identical λ_1 distributions, as FTLE depends only on (model, prompt, tangent seed, cadence).

Table 1: Model-to-condition mapping (locked from Escape Velocity).

Condition	Model	FTLE calls
HOMO_A	meta-llama/Llama-3.1-8B-Instruct (rev 0e9e39f2)	1,800
HOMO_B	Qwen/Qwen2.5-7B-Instruct (rev a09a3545)	1,800
HOMO_C	mistralai/Mistral-7B-Instruct-v0.3 (rev c170c708)	1,800
HETERO_ROT	meta-llama/Llama-3.1-8B-Instruct (rev 0e9e39f2)	1,800

2.4 Bridge analysis

Six preregistered Spearman rank correlations between three λ_1 summaries and two Escape Velocity collapse metrics:

- **λ_1 summaries:** mean λ_1 , layerwise profile variance, depth-profile slope.
- **Escape Velocity metrics:** collapse rate, first collapse turn (censored at 40 for non-collapsing), collapse incidence.

Multiple comparison correction: Bonferroni–Holm step-down across 6 tests, family $\alpha = 0.05$. Confidence intervals: bias-corrected bootstrap percentile (10,000 resamples, seed 42). Success criterion: ≥ 1 test with $|\rho| \geq 0.40$ and Holm-adjusted $p < 0.05$.

Sensitivity analysis repeated on the 167-window rater-agreed subset from Escape Velocity reliability audit.

3 Results

3.1 Phase 2 execution

All 7,200 FTLE calls completed with zero attrition (0 NaN/Inf, 0 failures). Wall time: 23.4 minutes. Estimated cost: \$20 (well under \$500 cap).

3.2 Bridge correlations

Table 2: Primary bridge results ($n = 720$). Prereg threshold: $|\rho| \geq 0.40$, Holm $p < 0.05$.

#	λ_1 summary	Escape Velocity metric	ρ	p_{Holm}	95% CI	Pass
1	mean	collapse rate	+0.246	4.26×10^{-11}	[+0.17, +0.32]	✗
2	mean	first collapse turn	-0.251	2.29×10^{-11}	[-0.32, -0.18]	✗
3	mean	collapse incidence	+0.036	0.337	[-0.03, +0.10]	✗
4	variance	collapse rate	+0.511	2.41×10^{-48}	[+0.45, +0.57]	✓
5	slope	collapse rate	-0.536	5.24×10^{-54}	[-0.59, -0.48]	✓
6	slope	first collapse turn	+0.507	1.22×10^{-47}	[+0.45, +0.56]	✓

Three of six tests pass: Tests #4, #5, and #6. The preregistered success criterion (≥ 1 pass) is met. The effect-size magnitudes ($|\rho| = 0.51\text{--}0.54$) are the primary evidence; the reported p -values are nominal and likely anti-conservative due to predictor non-independence (see Limitations). We interpret this as exploratory support for the bridge hypothesis under this protocol, not confirmatory relationship establishment or mechanistic validation.

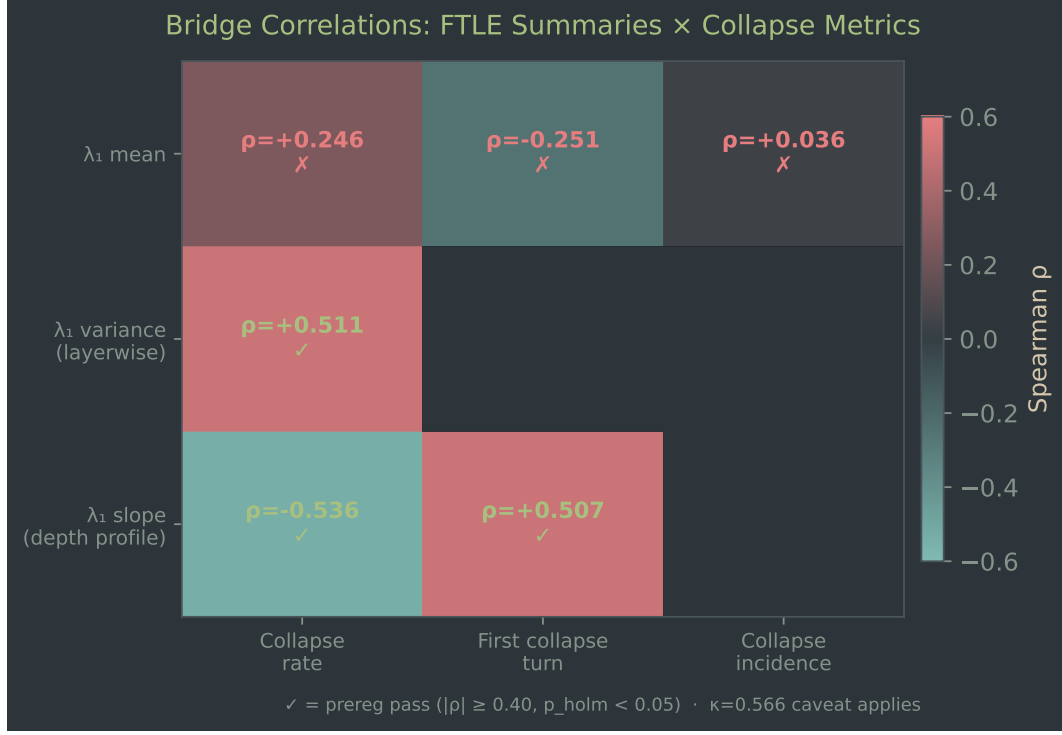


Figure 1: Bridge correlation heatmap. Checkmarks indicate tests meeting the preregistered threshold ($|\rho| \geq 0.40$, Holm $p < 0.05$). All correlations are subject to the Escape Velocity label reliability caveat ($\kappa = 0.566$).

3.3 Sensitivity analysis

Table 3: Sensitivity analysis ($n = 167$ rater-agreed subset).

#	λ_1 summary	Escape Velocity metric	ρ	p_{Holm}	Pass
1	mean	collapse rate	+0.255	1.75×10^{-3}	✗
2	mean	first collapse turn	-0.265	1.64×10^{-3}	✗
3	mean	collapse incidence	-0.005	0.947	✗
4	variance	collapse rate	+0.545	1.39×10^{-13}	✓
5	slope	collapse rate	-0.557	3.15×10^{-14}	✓
6	slope	first collapse turn	+0.516	3.86×10^{-12}	✓

The same three tests pass in the sensitivity analysis, with consistent effect sizes (within CIs of the primary analysis).

3.4 Depth profiles

4 Protocol corrections

Two deviations from PREREG_v2.md were identified and corrected before results were finalized:

1. **Test #4 variable mapping:** Initially used `lambda1_std` (tangent-seed standard deviation).

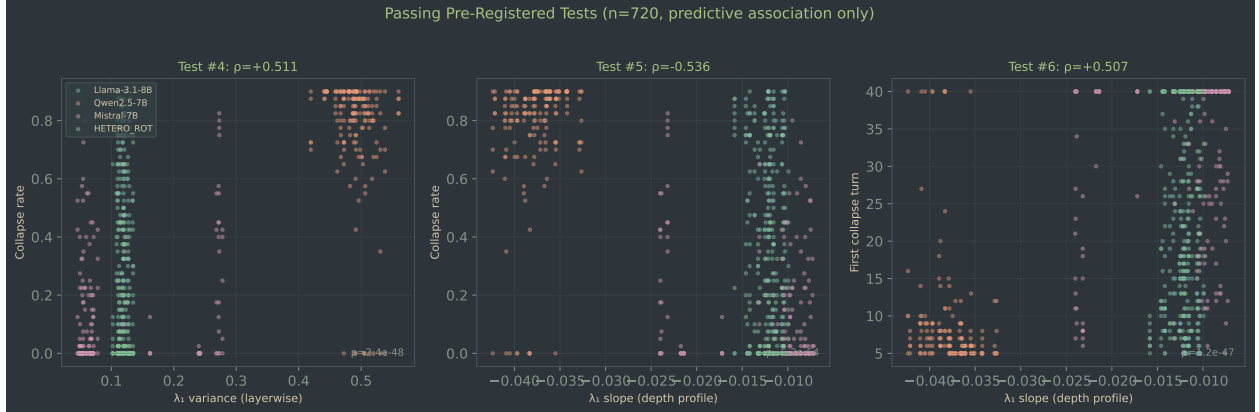


Figure 2: Scatter plots for the three passing tests. Colors indicate experimental conditions. Predictive associations only—no causal claims.

Corrected to `layerwise_variance_mean` (layerwise profile variance) per the preregistered definition. This changed ρ from -0.059 to $+0.511$ and promoted Test #4 from fail to pass.

2. **first_collapse_turn missingness:** Initially excluded non-collapsing runs ($n = 540$). Corrected to censor at turn 40 per the preregistered specification ($n = 720$). Test #6 attenuated slightly ($\rho: 0.539 \rightarrow 0.507$) but still passed.

Full before/after comparison is documented in `DEVIATION_TABLE.md`. The fact that Test #4 changed from fail to pass on correction warrants additional interpretive caution.

4.1 Candidate mechanisms (speculative)

The observed association between depth-profile features and collapse susceptibility is consistent with at least two broad hypotheses, neither of which is tested here:

- **Sensitivity compression:** Models whose depth dynamics concentrate sensitivity in early layers (steep negative slope) may have less capacity to differentiate contextually diverse inputs in later layers, producing more homogeneous outputs over extended interaction.
- **Architectural confound:** The three model families differ in architecture, training data, and alignment procedures. The observed λ_1 profile differences may reflect these model-level properties rather than a generalizable relationship between depth dynamics and collapse behavior. A within-model-family test (varying prompts or conditions while holding model constant) would be needed to distinguish these explanations; such a test is not available in the current design because each model family appears in only one or two conditions.

These remain hypotheses for follow-up investigation, not conclusions of the present study.

4.2 What this does not show

These results do not establish a causal mechanism linking within-forward-pass depth dynamics to across-turn conversational collapse. They also do not guarantee transfer beyond the tested model families and protocol choices. Finally, bridge effect sizes remain bounded by the Escape Velocity label-reliability limitation ($\kappa = 0.566$).

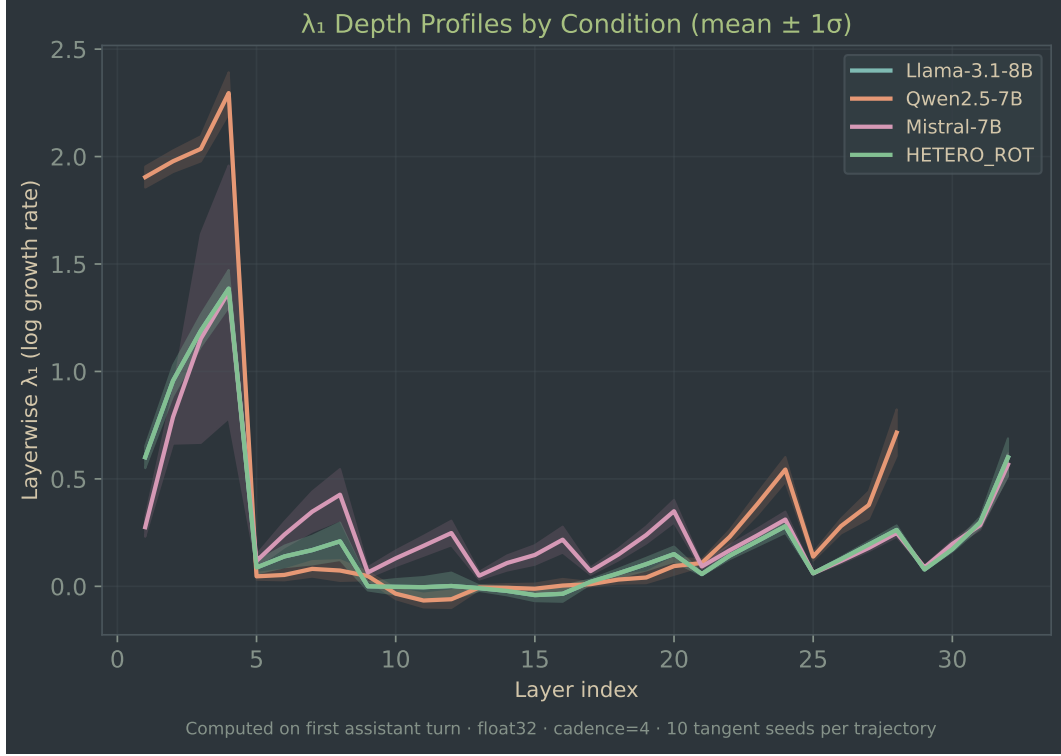


Figure 3: Mean λ_1 depth profiles by condition. The shape differences (slope, variance) drive the observed associations with collapse behavior.

5 Limitations

Escape Velocity label reliability. All bridge correlations use Escape Velocity collapse labels with unconfirmed inter-rater reliability ($\kappa = 0.566$, threshold 0.80 not met; raw agreement 92.8%). Effect sizes may be attenuated or inflated by label noise. The sensitivity analysis on 167 rater-agreed windows provides a partial check but not a full resolution.

Predictive association, not causation. λ_1 depth dynamics and conversational collapse operate on fundamentally different time axes (within-forward-pass vs. across-turn). The observed correlations indicate predictive association; no causal mechanism is established.

Mean λ_1 insufficiency. Three of six tests failed because mean λ_1 showed only weak associations ($|\rho| \leq 0.25$). The *shape* of the depth profile matters more than its average level.

Model family confound. HOMO_A and HETERO_ROT produce identical λ_1 distributions (both use Llama-3.1-8B). Between-model λ_1 variation may partially reflect architectural differences rather than a generalizable relationship.

Predictor dependence structure. HOMO_A and HETERO_ROT share the same model and seed prompts, producing identical λ_1 values for matched seeds. Additionally, within each condition, the five repeat trajectories per seed share identical λ_1 values (FTLE depends only on model, prompt, tangent seed, and cadence). Consequently, the 720-row bridge analysis contains only 108

unique λ_1 vectors (36 seeds \times 3 distinct models), each repeated across multiple rows with different Escape Velocity collapse outcomes. The within-cluster collapse variance drives the observed correlations, but the non-independence of the predictor means effective degrees of freedom are lower than the nominal $n = 720$. Standard errors are likely underestimated and the reported p -values and confidence intervals should be interpreted as anti-conservative. The preregistered protocol specified $n = 720$ with these conditions, so we report the planned analysis but flag this structural dependence as a limitation on inferential precision.

Precision sensitivity. Float64 and float32 λ_1 estimates are not interchangeable ($r = 0.788$). All production runs used float32 consistently.

Single first-turn measurement. λ_1 is computed on the first assistant turn only. A longitudinal study computing λ_1 at each turn could provide stronger evidence but was out of scope.

6 Conclusion

We observe that λ_1 *profile features*—depth-profile slope and layerwise variance—show medium-to-large associations with multi-turn collapse behavior ($|\rho| = 0.51\text{--}0.54$) across three 7B-parameter model families. Mean λ_1 alone is insufficient. These results are consistent with the hypothesis that the shape of a model’s depth-dynamics sensitivity profile is informative about collapse susceptibility, but the evidence is exploratory rather than confirmatory: the predictor dependence structure (108 unique vectors across 720 rows) means nominal p -values overstate statistical certainty, and the between-model-family design cannot distinguish depth-dynamics effects from model-level confounds.

The primary durable contribution is the FTLE profiling pipeline itself: a computationally tractable, numerically stable method for estimating depth-dynamics sensitivity in production-scale transformers ($\$20$ for $7,200$ calls). The bridge evidence provides a testable direction for future work, not a confirmed relationship.

All findings carry the Escape Velocity label reliability caveat ($\kappa = 0.566$) and are restricted to observed associations under the tested protocol. The highest-priority follow-ups are: (1) human-rater reliability validation for Escape Velocity labels; (2) dependency-aware inference (e.g., clustered bootstrap at the seed \times model level); and (3) within-model-family tests using diverse prompt sets to separate model-level from prompt-level variation.

References

- Atilim Gunes Baydin, Barak A Pearlmutter, Alexey Andreyevich Radul, and Jeffrey Mark Siskind. Automatic differentiation in machine learning: a survey. *Journal of Machine Learning Research*, 18(153):1–43, 2018.
- Ricky TQ Chen, Yulia Rubanova, Jesse Bettencourt, and David Duvenaud. Neural ordinary differential equations. In *NeurIPS*, 2018.
- Jean-Pierre Eckmann and David Ruelle. Ergodic theory of chaos and strange attractors. *Reviews of Modern Physics*, 57(3):617, 1985.
- Ari Holtzman, Jan Buys, Li Du, Maxwell Forbes, and Yejin Choi. The curious case of neural text degeneration. *arXiv preprint arXiv:1904.09751*, 2019.

Jiwei Li, Michel Galley, Chris Brockett, Jianfeng Gao, and Bill Dolan. A diversity-promoting objective function for neural conversation models. *arXiv preprint arXiv:1510.03055*, 2016.

Sean Welleck, Ilia Kulikov, Stephen Roller, Emily Dinan, Kyunghyun Cho, and Jason Weston. Neural text generation with unlikelihood training. In *ICLR*, 2020.

Alan Wolf, Jack B Swift, Harry L Swinney, and John A Vastano. Determining Lyapunov exponents from a time series. *Physica D: Nonlinear Phenomena*, 16(3):285–317, 1985.